



UNIVERSITÀ POLITECNICA DELLE MARCHE  
Repository ISTITUZIONALE

Pauli principle and the Monte Carlo method for charge transport in graphene

This is a pre print version of the following article:

*Original*

Pauli principle and the Monte Carlo method for charge transport in graphene / Coco, M., B ordone, P., Demeio, L., Romano, V.. - In: PHYSICAL REVIEW. B . - ISSN 24 69-9969. - 104 :20(2021).  
[10.1103/PhysRevB .104 .2054 10]

*Availability:*

This version is available at: 11566/29934 4 since: 2024 -11-22T14 :13:13Z

*Publisher:*

*Published*

DOI:10.1103/PhysRevB .104 .2054 10

*Terms of use:*

The terms and conditions for the reuse of this version of the manuscript are specified in the publishing policy. The use of copyrighted works requires the consent of the rights' holder (author or publisher). Works made available under a Creative Commons license or a Publisher's custom-made license can be used according to the terms and conditions contained therein. See editor's website for further information and terms and conditions.

This item was downloaded from IRIS Università Politecnica delle Marche (<https://iris.univpm.it>). When citing, please refer to the published version.

(Article begins on next page)

# **Dynamic performance of a full-scale micropile group: Relevance of nonlinear behaviour of the soil adjacent to micropiles**

Maria Chiara Capatti<sup>a</sup>, Francesca Dezi<sup>b1</sup>, Sandro Carbonari<sup>a</sup>, Fabrizio Gara<sup>a</sup>

<sup>a</sup> Department of Construction, Civil Engineering and Architecture, DICEA, Università Politecnica delle Marche, Via Brecce Bianche, 60131 Ancona, Italy. E-mail: m.c.capatti@pm.univpm.it, s.carbonari@univpm.it, f.gara@univpm.it

<sup>b</sup> Department of Economics, Science and law, DESD, University of San Marino, Via Consiglio dei Sessanta, 99, 47891, Republic of San Marino. E-mail: francesca.dezi@unirmsm

## **Abstract**

An extensive experimental in-situ campaign of dynamic tests carried out on a full-scale 2 x 2 group of inclined injected micropiles in alluvial soils is described in this paper. The campaign includes ambient vibration and impact load tests to investigate the dynamic behaviour of the soil-micropile system in the small strain range, and forced vibration tests to investigate the performance of the system in the nonlinear field. Accelerometers and geophones are adopted to acquire the dynamic response on the cap and the soil nearby the cap, while strain gauges are installed along the shaft of one micropile to capture the local curvatures and deflections. The influence of the micropile inclination on the translational and rotational behaviour of the group is evaluated. Moreover, the evolution of degradation phenomena such as the gap opening and slippage at the soil-micropile interface and the radial cracking of soil surrounding micropiles, are recognized, critically commenting the relevant effects on the fundamental frequencies and damping ratios of the system.

*Keywords:* Dynamic tests; In situ full-scale tests; Inclined micropile group; Soil-micropile non-linear interaction; Soil-pile gap.

---

<sup>1</sup> Department of Economics, Science and law, DESD, University of San Marino, Via Consiglio dei Sessanta, 99, 47891, Republic of San Marino. - Tel.: + 39 0549 888111, E-mail address: E-mail: francesca.dezi@unirmsm

## 1 Introduction

In seismic areas, the use of micropiles for foundations of new constructions and for the retrofit of existing structures (i.e. old buildings, bridges) is growing up. Regarding the latter field of application, micropiles can be connected around or below the existing foundation not only vertically, but even in inclined arrangement (groups or networks of inclined micropiles). Inclination increases the overall horizontal resistance of the soil-foundation system and micropiles behave similarly to tree roots. Alongside, theoretical and experimental studies aiming at improving the knowledge about the behaviour of micropiles under dynamic horizontal loading are increasing; those studies mainly focus on the behaviour of vertical small-diameter piles, neglecting the role of executive techniques (such as high-pressure injections, realized for Tubfix micropiles and other common micropile technologies) and inclined layouts. Inclined piles and micropiles can resist high lateral loads by exploiting their axial behaviour. However, from the observations of past case histories, the behaviour of inclined large-diameter piles turns out to be ambiguous. Damage of battered piles were observed, for instance, after the 1989 Loma Prieta earthquake at the port of Oakland and San Francisco (SEAOC, 1991) or after the 1991 Costa Rica earthquake in the front batter piles of the Rio Banano bridge and in piles of the Rio Vizcaya Bridge (Priestley et al., 1991). The presence of severe cyclic forces at the pile cap and the degradation of bending moment capacity due to seismically induced tensile and shear forces are some of the reasons identified by Giannakou et al. (2010) for such disadvantageous behaviour. On the other hand, case histories referring to Maya Wharf in the Kobe 1995 earthquake and the Landing Road Bridge in the Edgecumbe in the New Zealand 1987 earthquake, have highlighted the successful performance of battered piles. Nonetheless, the use of inclined piles is still not recommended by modern European codes (i.e. AFPS 90, EN1998-5, NTC 2018).

To improve the knowledge about the seismic response of batter piles and micropiles, both numerical and empirical studies were carried out recently. Bruce et al. (1995), Sadek and Isam (2004), Sadek and Shahrour (2006), Gerolymos et al. (2008), Padron et al. (2009) and Dezi et al. (2016a), just to cite a few, have shown that, under the assumption of linear or linear equivalent soil behaviour and perfect adherence at the soil-micropiles interface, the response of well-designed batter piles can be beneficial for the structure they support (González et al., 2019a, b) and for the foundation itself Carbonari et al. (2017).

From the experimental point of view, the state of the art is mainly based on reduced scale experiments in dry sand: Juran et al. (2001) made a series of centrifuge tests in loose to dense dry Nevada sand, investigating small diameter polystyrene pile groups and network systems, as well as the superstructure soil-pile interaction behaviour. Tests indicate a positive group effect, increasing with the number of piles and the batter angle, and lead to softer dynamic p-y curves than those available in the literature. A substantial improvement is also observed in the superstructure response. Escoffier et al. (2008) performed reduced scale centrifuge tests to compare the dynamic behaviour of a 1x2 vertical pile group and a 1x2 group with one inclined pile embedded in dry Fontainebleau sand, under horizontal repeated impact load tests. Results highlighted the presence of a translational-rocking mode of vibration of the rigid cap, for which the inclined group was stiffer than the vertical one. The inclined pile induced a decrease of the translational movement of the cap, a decrease in the maximum bending moment below the soil surface in both piles with respect to the vertical pile group, and an increase of the maximum bending moment at the pile-cap interface in the rear pile. Finally, the axial force was significantly increased in both the front and rear pile of the inclined pile group.

Concerning full scale experiments on micropiles in more realistic soil conditions, Abd Elaziz and El Nagggar (2014) performed monotonic and cyclic lateral load tests on four hollow bar micropiles in cohesive soils but did not investigate the dynamic behaviour nor inclination.

Concerning the dynamic behaviour, full-scale tests in both cohesive and granular soil focused mainly on vertical piles and pile groups (i.e. Novak and Grigg, 1976; Kobori et al., 1991; El Marsafawi et al., 1992; Tuzuki et al., 1992; Imamura et al., 1996; Dezi et al., 2012, 2013 and 2016b and Pender et al., 2018); more recently, Bharathi et al. (2019) presented an experimental investigation of vertical and batter pile groups in silty sands.

Overall, there is a lack of experiments on the dynamic behaviour of real scale inclined micropiles addressing the linear and nonlinear response of the soil-foundation system. Aspects deserving attention are the nonlinearities evolving in the soil and at the soil-pile interface.

In this framework, Capatti et al. (2018), performed full scale dynamic tests on injected and not injected single vertical micropiles embedded in alluvial soils to investigate the system performance in the linear and nonlinear fields, considering the role of the two executive techniques.

In this paper, an experimental campaign is carried out on a group of inclined injected micropiles in transitional silty soils, adopting different dynamic testing techniques to investigate the response under different dynamic loading conditions. Ambient Vibration (AV) tests and Impact Load (IL) tests are adopted to investigate the system in the small strain level, while Forced Vibration (FV) tests with increasing intensity of the applied dynamic force are adopted to determine the dynamic properties of the system at higher strain level. Results are shown in the frequency domain to point out the dynamic properties of the soil-foundation system, i.e. fundamental frequencies and damping ratios.

## **2 Geotechnical properties of the site and characteristics of the inclined micropile group**

### *2.1 Site description*

The test field is localized in the industrial area of San Biagio (Osimo), in central Italy. The area, characterized by a flat morphology, rests above a recent continental covering silty soil that mainly consists of eluvial-colluvial and Plio-Pleistocene alluvial deposits over a Plio-Pleistocene marine deposit prevalently composed of Pleistocene marly clays, locally layered with lenses of gravels and sands in clayey-silty matrix. The geotechnical model is summarized in Figure 1a. A geotechnical and geophysical survey was performed before the execution of the micropiles, including boreholes, field inspection tests (e.g. vane test and pocket penetrometer), laboratory tests (e.g. triaxial test), in-situ tests conducted up to a maximum depth of about 20 m (e.g. Cone Penetration Test - CPT) and geophysical tests (e.g. Multichannel Analysis of Surface Waves - MASW, Extended Spatial AutoCorrelation – ESAC, Horizontal to Vertical Spectral Ratio - HVSR).

Ground Water Level (GWL) was about 3.5 - 4.0 m below the ground surface and during the tests it was periodically checked by means of an open standpipe piezometer installed in the close proximity of the micropile foundation.

The portion of soil interested by the presence of the micropiles (i.e. up to a depth of 7.5 m) is constituted by a normally consolidated alluvial silty layer with poor mechanical properties. Figure 1b summarizes the location of the main tests, while Figure 1c and Figure 1d show, up to a depth of 10 m, the cone resistance  $q_c$  profile from CPT data, and the profile of shear wave velocity  $V_s$  as obtained from geophysical survey and from correlation with  $q_c$  values. The average  $V_s$  in the portion of soil interested by the presence of micropiles is about 180 m/s.

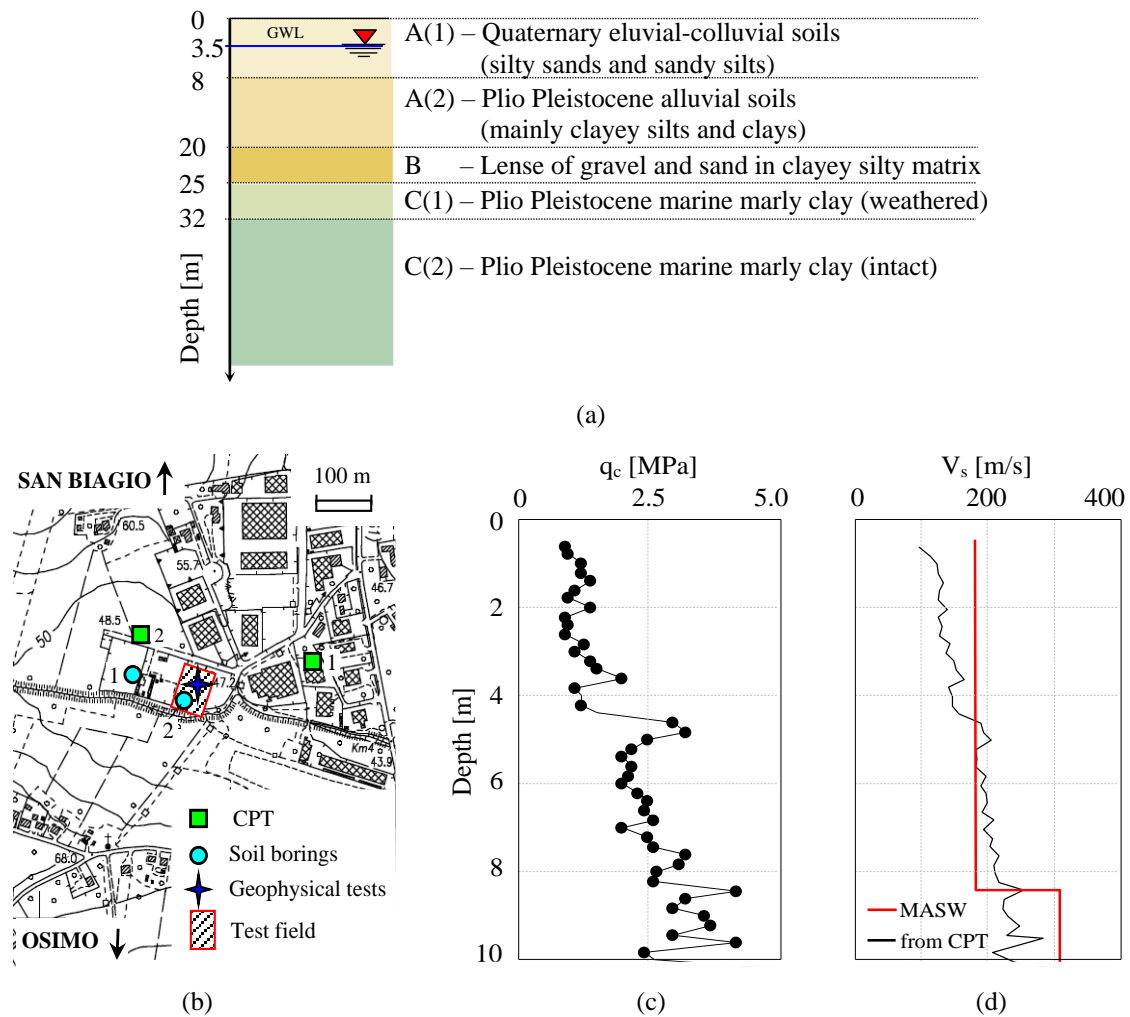


Figure 1. (a) Geotechnical model; (b) location of the test field and geotechnical surveys; (c)  $q_c$  and (d)  $V_s$  profiles.

## 2.2 Inclined micropile foundation

The investigated foundation system is a 2x2 group of inclined Tubfix micropiles. The reinforcement of micropiles is constituted by four 2 m long steel pipe elements connected by means of threaded female pipe couplers. The cross section of each pipe has an outer diameter of 76.1 mm and thickness of 6 mm. The 3<sup>rd</sup> and 4<sup>th</sup> element from the top of the micropiles are equipped with four 50 cm spaced valves a manchèttes for high pressure injections; the 4<sup>th</sup> element is also provided with a bottom plug for a high-pressure grout injection at the micropile tip. For one of the micropiles, the assembly of the steel elements was done in laboratory to allow the proper installation of permanent instrumentation along the pipe. Once the sensors

were mounted and carefully protected, the pipes were transported in situ for the installation. First, the soil drilling was performed with a diameter of 170 mm, an angle of inclination to the vertical axis of  $15^\circ$  and a total (inclined) length of 7.5 m. The inclination was given only around the  $x$  axis, i.e. along the  $y$  axis, with respect to the right handed orthogonal reference system indicated in Figure 2a, where a schematic plan view of the testing field is also provided; in this way the geometrical configuration turned out to be symmetrical with respect to the  $z$ - $x$  plane. Then, drilling rods were removed and bores were filled with the first grouting. Immediately after, pipes were carefully inserted and 48 hours later, additional neat grout was injected (at a pressure of 6 - 8 MPa) through the valves a manchèttes in all the micropiles using a packer with double effect piston (Figure 2b).

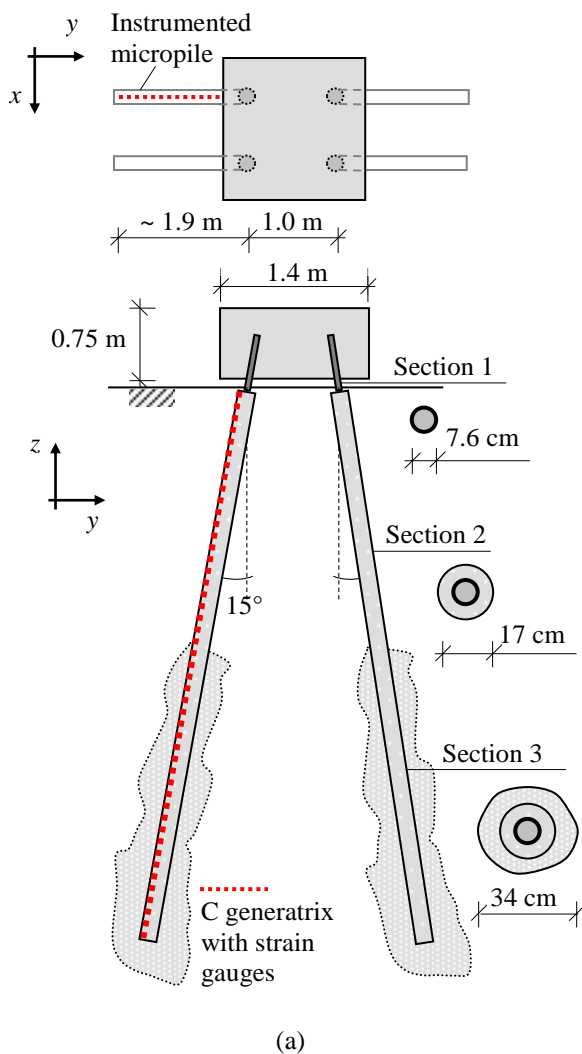


Figure 2. (a) Plan and lateral view of the foundation; (b) from the top to the bottom: high pressure injections,

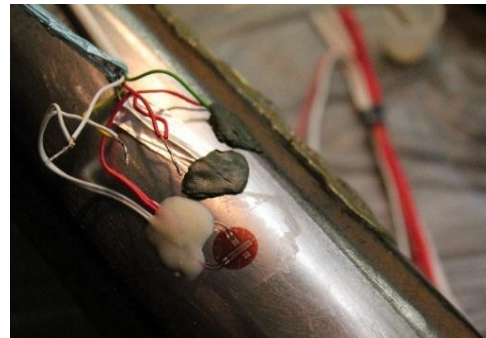
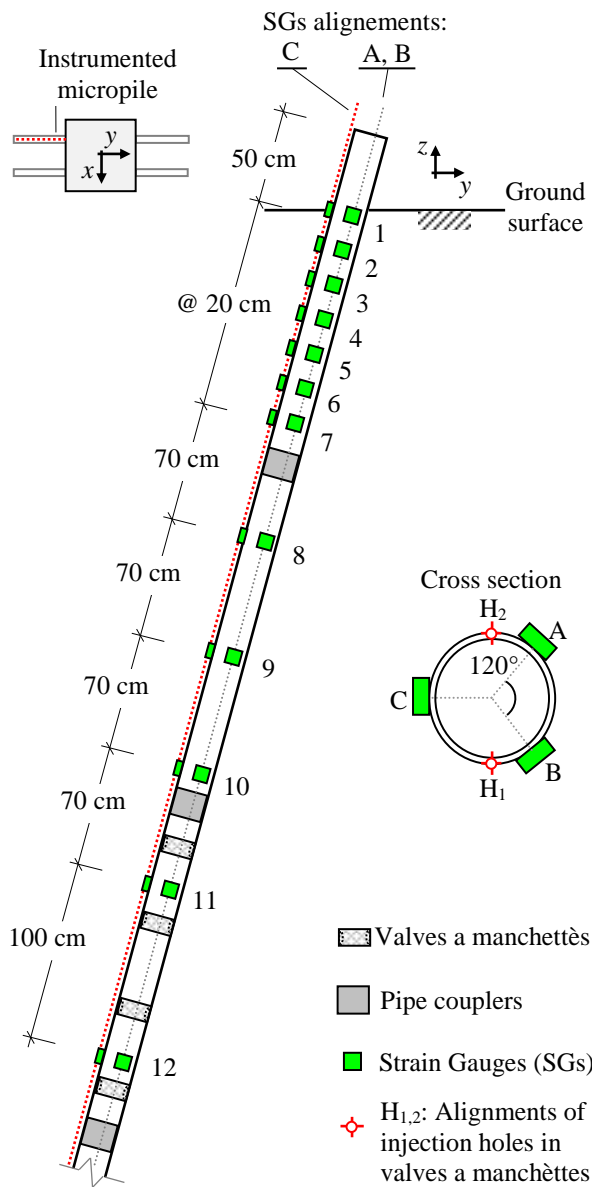
view of the four inclined micropiles before and after the cap execution.

The cement slurry used for both the first and the secondary (selective) grouting had a water cement ratio of 0.5. The quantity of cement slurry injected during high-pressure injections was calculated to obtain an equivalent diameter in the injected portion of the micropile equal to 2 times the diameter of the borehole. The elastic modulus of the concrete adopted for the micropiles execution (used for both the first grouting and the high-pressure injections) was 22000 MPa as obtained from the results of ultrasonic tests. A view of the four inclined micropiles after the injections is provided in Figure 2b. Finally, a concrete cap (1.4 m x 1.4 m x 0.75 m) was realized at the micropiles head (Figure 2) avoiding the contact between the ground surface and the cap through a polystyrene sheet. Cap dimensions are defined to assure an adequate flexural stiffness to satisfy the hypothesis of rigid connection at the pile heads and to get fundamental frequencies of the soil-micropile system below 50 Hz, which is the highest operating frequency of the vibrodyne adopted for executing the forced vibration tests of the experimental campaign.

### *2.3 Permanent Instrumentation*

For the measurement of longitudinal strains and curvature along the pipe, one of the inclined micropiles was equipped with a total of 36 strain gauges (SGs) installed along 3 generatrices (A, B, C) equally spaced along the cross-sectional circumference, as shown in Figure 3. As well known, under the assumption that cross sections remain plane after bending, this disposition allows the determination of strains within the whole cross section (i.e. curvatures about principal axes and neutral axis). To avoid as much as possible damage on SGs on the generatrix C due to injections, and to facilitate the interpretation of results, holes of valves a manchèttes were aligned along two generatrices (H1, H2)  $\pm 90^\circ$  spaced from the generatrix C (indicated with a red dotted line in Figure 3a). The alignment of SGs on generatrix C is considered as the main one and the instrumented micropile was mounted and installed in such

a way that the generatrix C is oriented upward. The number and layout of sensors along the steel pipe were defined through results of a preliminary numerical soil-micropile interaction analysis. T-rosettes SG with two measuring steel grids connected in a half-bridge configuration were used, to avoid thermal effects (Figure 3b). Each SG has a gauge resistance of 120 Ohm and a gauge length of 5 mm.



(a)

(b)

Figure 3. (a) Layout of SGs on the instrumented micropile; (b) installation of SGs, cables soldering, and protection.

Special attention was devoted to the protection of sensors and cables against mechanical stresses induced by the high-pressure injections along the shaft of the steel core, as well as against aggressive agents (moisture and weathering above all) (Figure 3b). Moreover, each SG is protected, both chemically and mechanically, with specific polyurethane paint and aluminium foil coupled with kneading compound; cables placed near valves a manchèttes are protected with high-resistance corrugated polyethylene pipes. Preliminary tests, performed before and after the execution of the injections, prove that most of the permanent sensors worked properly after the installation of the instrumented steel core as well as after the high-pressure injections.

In addition to the permanent instrumentation above described, other measuring devices were used depending on the executed test and will be described in the following.

### **3 Experimental campaign**

The experimental program on the micropile group started in August 2016 and ended in October 2017. Preliminary AV tests were performed on one of the inclined micropile, after the execution of high pressure injections and maturation of the grout. Once the cap was executed, IL tests were carried out at the beginning of August 2016 to investigate the response of the group in the small strain range. At the end of August 2016 AV tests with geophones were carried out to investigate the dynamic behaviour of the system to ambient noise (very small strain range). It is worth mentioning that this test was performed after the beginning of a seismic sequence that hit central Italy starting from August 24<sup>th</sup> 2016 (Central Italy earthquake). In September 2016 FV tests with a vibrodyne were carried out to investigate the behaviour of the soil-foundation system in the medium-to-high strain range. The variation of the dynamic properties of the system immediately after and one year after the execution of FV tests were

monitored by means of IL tests. In Table 1 the sequence of the performed tests is briefly reported.

Table 1. Synthetic sequence of the tests performed on the foundation.

Date	05/08/2016	26/08/2016	07/09/2016	05/10/2017
Test	IL	AV	FV and IL	IL

### *3.1 Impact load tests*

IL test is a typical test for identifying the dynamic properties of a system in a wide range of frequencies with few blows of an instrumented hammer and short acquisition times. However, since a low amount of input energy is supplied to the system at each frequency, this method is usually useful for analysing the dynamic properties of small systems in the range of very small to small/medium strains. In this sense, it is not usually suitable to investigate system nonlinearities which generally occur at higher strain levels.

For this test, the additional instrumentation consists of seven uniaxial accelerometers positioned on the micropile cap as shown in Figure 4a. Piezoelectric accelerometers with a sensitivity of about 10 V/g, a frequency range ( $\pm 10\%$ ) of 0.07 - 300 Hz, and a broadband resolution of 1  $\mu\text{g}$  rms were used; accelerometers were mechanically connected to small plates bonded to the cap surface by means of hot melt glue or quick-setting glue. The measuring chain also included an instrumented large-sledge impulse hammer having a mass of 5.5 kg, equipped with a load cell with maximum capacity of 22 kN and sensitivity of 0.23 mV/N. The sensors were connected to the power supply and a 24-bit Data Acquisition (DAQ) system having an input range of  $\pm 5$  V through low-noise coaxial cables. Therefore, the acquisition system is able to measure accelerations up to  $\pm 0.5$  g. Finally, a laptop with dedicated software was used for storing and processing the registered signals. A sampling frequency of 2048 Hz was chosen to

achieve high resolution in time domain, while the acquisition time duration was of 2 s for each IL test.

The micropile foundation system is expected to behave differently along  $x$  and  $y$  axes, as a consequence of the unilateral inclination of micropiles. The coupled roto-translational dynamic behaviour of the system in the  $x$ - $z$  and  $y$ - $z$  planes is fully investigated, as well as the likely coupled torsional-translational behaviour in the  $x$ - $y$  plane, triggered by accidental asymmetry of the system. Accordingly, 3 different test configurations were considered, along both  $x$  and  $y$  axes, while 8 configurations were adopted along the vertical direction (for a total of 14 test configurations). For each configuration at least 5 impacts were executed to check the repeatability of the results and to get a reliable average response. Figure 4b provides a schematic representation of all the IL tests carried out on the soil-micropile foundation system along the three directions  $x$ ,  $y$ , and  $z$ .

In Figures 5 and 6 results of IL tests are reported along  $x$ ,  $y$ , and  $z$  axes. Responses of accelerometers are shown in terms of Frequency Response Function (FRF), i.e. the ratio between the Fourier transform of the output (i.e. acceleration signals) and the Fourier transform of the input (i.e. the hammer impact signal). By identifying the peaks of FRF, it is possible to detect the fundamental frequencies of the system, while from the width of the peaks an estimate of the damping ratios can be obtained by adopting the half power bandwidth method. Finally, information about the mode shape associated to the fundamental frequencies can be obtained from amplitude values. Results of IL tests are shown in terms of mean values resulting from all the impacts for each configuration.

In Figure 5a results of tests performed along  $x$  direction (ILx1, ILx2 and ILx3) are shown with 3 rows of plots, each one relevant to FRFs of accelerations measured along  $x$ ,  $y$  and  $z$  directions.

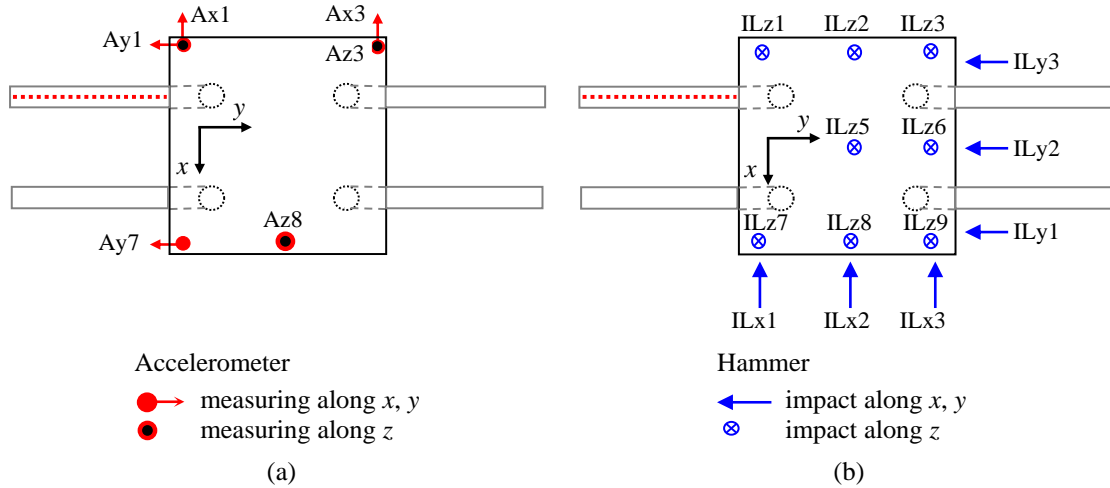


Figure 4. (a) Layout of accelerometers on the micropile cap and (b) point and direction of impacts.

Accelerometers acquiring along  $x$  axis (i.e. Ax1 and Ax3) show, in the investigated range of frequencies, two resonance peaks: the first, at 38.5 Hz, is stable in all the configurations and corresponds to the first translational mode of vibration of the foundation along  $x$  axis ( $f_{l,x}$ ); the second, which is more pronounced for the configurations with eccentric impacts (ILx1 and ILx3) and only slightly evident for impact ILx2, is approximately at 60 Hz and is mainly related to a torsional mode around the  $z$  axis ( $f_{l,y}$ ). Anyway, the torsional mode is coupled with the translational one in the  $x$  direction, as can be observed from the FRFs relevant to sensors A1x and A2x, which are slightly different in terms of amplitude; the coupling is due to an accidental asymmetry of the system probably due to the heterogeneity of the soil deposit and the non-uniformity of the injected portion of micropiles. By observing the response of the accelerometers acquiring along the vertical direction for all the investigated configurations of impact, it is evident that both the translational and the torsional modes are coupled with the rocking mode of vibration along  $y$  direction as demonstrated by clear peaks in FRFs of accelerations in the vertical directions at both 38.5 Hz and 60 Hz (marked with black and red dotted lines, respectively). Finally, it is worth noting that while peaks of the two vertical accelerations at 38.5 Hz have equal amplitude, those relevant to 60 Hz are different, revealing that the centre of rotation around the  $y$  axis is not exactly centroidal.

In Figure 5b results of tests performed along  $y$  direction are shown (ILy1, ILy2 and ILy3). As previously, FRFs are collected in three rows, each one relevant to a direction of acquisition of the accelerations. Consistently with what observed along  $x$  direction, all accelerometers show a peak in the FRFs at about 60 Hz (i.e. roto-translational mode of vibration in the  $x$ - $y$  plane), while the first translational mode along  $y$  direction ( $f_{t,y}$ ) is particularly evident in test ILy2 at 45.5 Hz (marked with light blue dotted lines).

By observing the response of the accelerometers acquiring along the vertical direction, it can be noted that the rocking motion is coupled with the translational one at 60 Hz, while the coupling appears to be absent for the translational mode at 45.5 Hz. This phenomenon is in line with that observed by Carbonari et al. (2017), in case of inertial loads acting on inclined pile groups. In details, for inclined pile group foundations loaded by a horizontal force also producing bending moment in the pile inclination plane (like in the performed tests where the impact is applied at the top of the pile cap), the cap rotation results from the contribution of two opposite effects, relevant to the bending moment and the shear force. Superposition of the above mentioned contributions, which are opposite in phase, is responsible for the obtained experimental data (absence of peak in the FRFs of the vertical response at 45.5 Hz), which only apparently suggests the absence of coupling. It is worth mentioning that for vertical piles, or for inclined ones loaded orthogonally to the pile inclination plane, contributions to the pile cap rotations due to bending moment and shear force are of the same sign (Carbonari et al., 2017, Giannakou et al., 2010).

In Figure 6 main results of some IL tests performed along  $z$  direction are shown. The previously identified coupled roto-translational behaviours (that involves vertical movements of the cap) are evident from the selected configurations. On the contrary, a pure vertical mode is not found within the investigated range of frequencies.

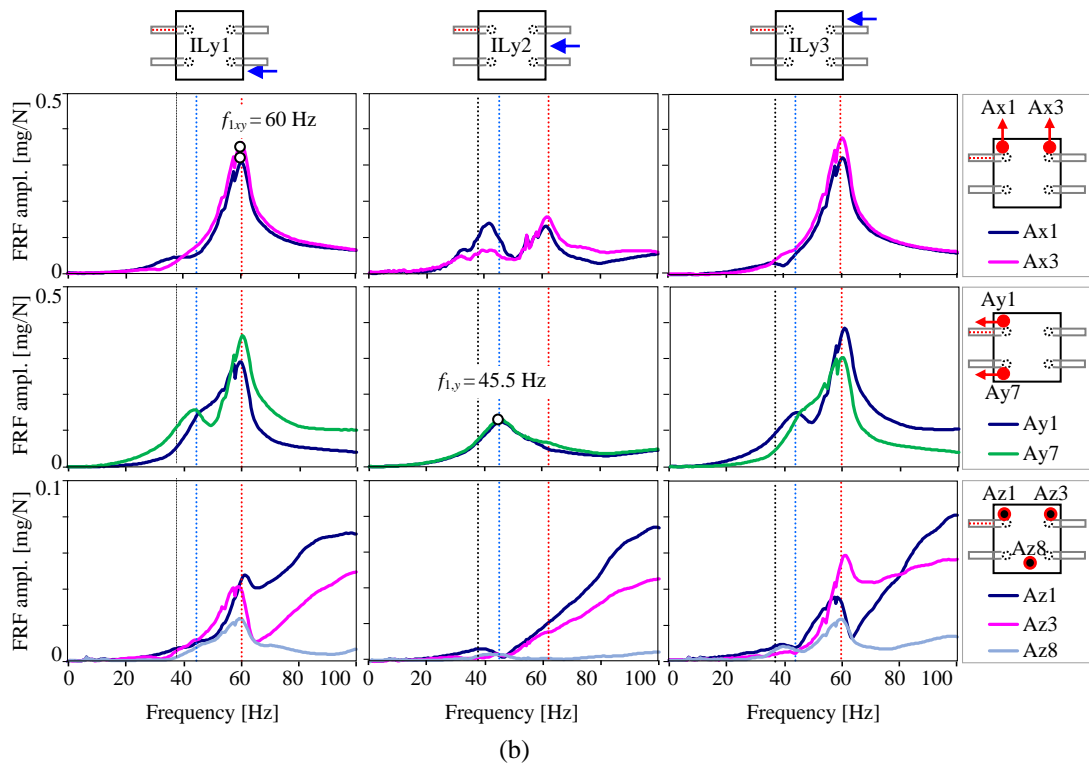
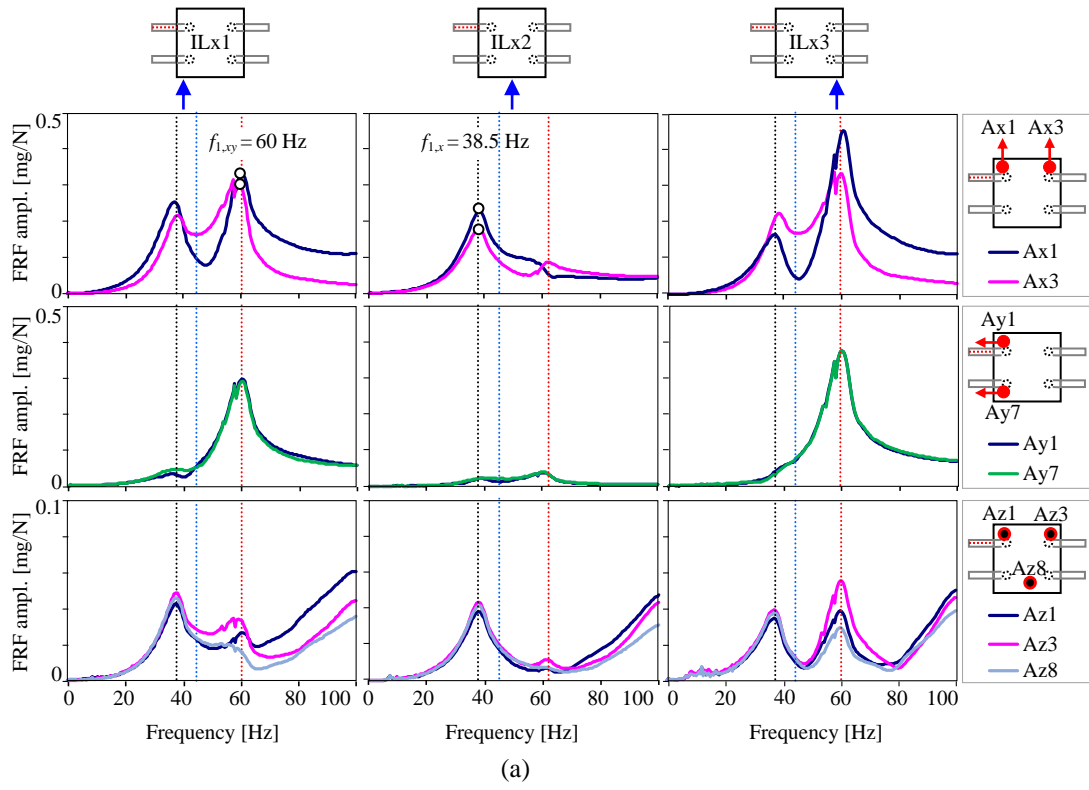


Figure 5. Results of IL tests in (a)  $x$  and (b)  $y$  directions.

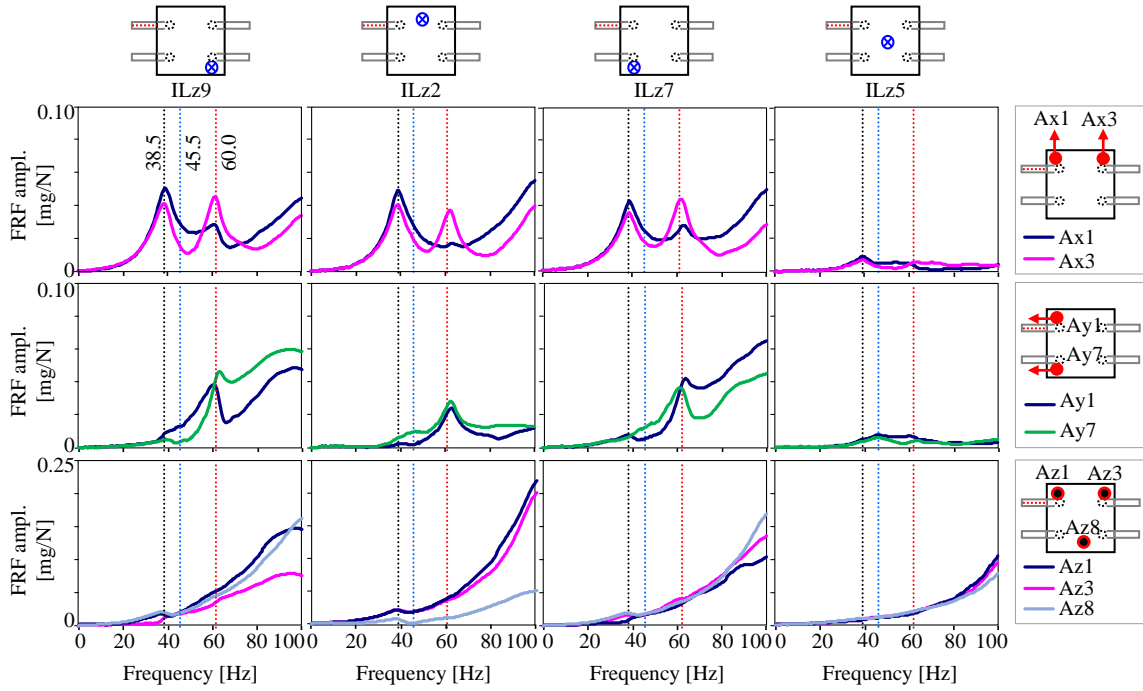


Figure 6. Results of IL tests in vertical directions.

Table 2 summarizes the fundamental frequencies identified through signals of accelerometers Ax1, Ax3 and Ay1, Ay7 from tests ILx2 and ILy2, respectively, and the relevant damping ratios obtained via the half-power bandwidth method. As expected, the soil-foundation system is sensibly stiffer along the direction in which micropiles are inclined (y axis), presenting a fundamental frequency about 18% higher than that in the  $x$  direction; also, damping ratio of the translation mode in the  $y$  direction is 30% higher than that in the  $x$  direction.

Table 2. Fundamental frequencies and damping ratios of the translational modes of vibrations from IL tests.

Test configuration	ILx2		ILy2	
Accelerometer	Ax1	Ax3	Ay1	Ay7
Fundamental frequencies [Hz]	38.5	38.5	45.5	45.5
Damping ratios [%]	10.3	9.6	12.7	13.3

### 3.2 Ambient vibration tests

AV tests are commonly adopted to identify the dynamic properties of various full-scale structures in the elastic range, at very small strain level, by measuring the response of the

system subjected to ambient noise (i.e. wind, anthropic activities, micro tremors and noise). Instead of using accelerometers (not enough sensible to catch the response of the capped foundation under ambient noise), AV tests on the micropile group were performed by means of two triaxial synchronized geophones (velocimeters) having a natural resonance frequency of 2 Hz ( $\pm 10\%$ ), and a sensitivity of 2 V/cm/s ( $\pm 5\%$ ). A dedicated software and a laptop were used for the acquisition and post processing of signals. Sensors were placed in four different configurations as shown in Figure 7: a geophone is always located on the ground surface (*Gff*), away from the cap, while the other one at different positions on the cap (*G1*, *G3*, *G5* and *G7*). In all the cases, a time length of about 1500 s and a sample frequency of 200 Hz were used for the acquisitions.

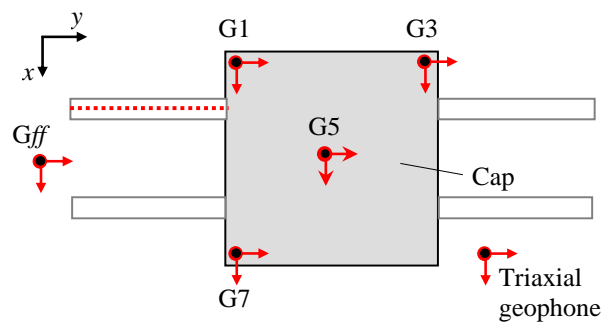


Figure 7. Layout of geophones for the different configurations of AV tests.

In Figure 8 results of tests are shown in terms of ratio between the frequency spectrum of velocity obtained on the cap and that obtained on the ground, to identify the fundamental frequency of the soil-foundation system through the observation of peaks. Due to the characteristics of the adopted geophones, the frequency range in which results can be well appreciated is within 50 Hz (lower than that obtained with IL tests).

In all the graphs, green and magenta dotted straight lines are used to mark the fundamental frequencies along *x* and *y* axes, respectively. Dealing with the first (flexural) mode of vibration, the behaviour of the system along the direction of micropiles inclination (*y*) is significantly

stiffer, and more damped than that along  $x$  direction, in line with previous results, as can be deduced observing the peak in the  $x$  direction, which is associated to a lower frequency and is characterised by a higher amplitude and a lower width than that in the  $y$  direction.

It can also be observed that fundamental frequencies (36.0 Hz and 42.5 Hz in the  $x$  and  $y$  directions, respectively) are slightly lower (about 6.5% in both  $x$  and  $y$  directions) than those previously measured with IL tests, despite AV tests usually provides higher frequencies than those obtained with other experimental methods, consistently with the very small strains induced by ambient vibrations. This peculiar behaviour may be ascribed to the fact that IL and AV tests were performed in different periods of the experimental campaigns, during the summer of 2016 (Table 1). Therefore, slight variations of the soil behaviour induced by rain, temperature changes and other atmospheric agents could have occurred; moreover, the two tests were respectively performed before and immediately after the Central Italy earthquake (2016) (Sextos et al., 2018). This can be responsible for the developing of certain non-linear phenomena in the soil-micropile system (e.g. soil stiffness degradation, sliding and detachment at the soil-micropile interface, especially in the shallower portion of the micropile) and, consequently, for a decrease in the fundamental frequency of the system. In this line, results from IL tests are representative of the initial tangent behaviour, while results from AV tests will be assumed as reference for interpreting results of subsequent tests.

### *3.3 Forced vibration tests*

FV test is the best technique to provide an input with high energy content and allows for an accurate assessment of the characteristics of the system also for highly damped modes that are not easy to catch with an IL test or a snap back test (that usually excite mainly the first mode of vibration). However, the test has a long duration and is generally considered unattractive due to the cost of the rental or purchase of the shaker, and to its transportation.

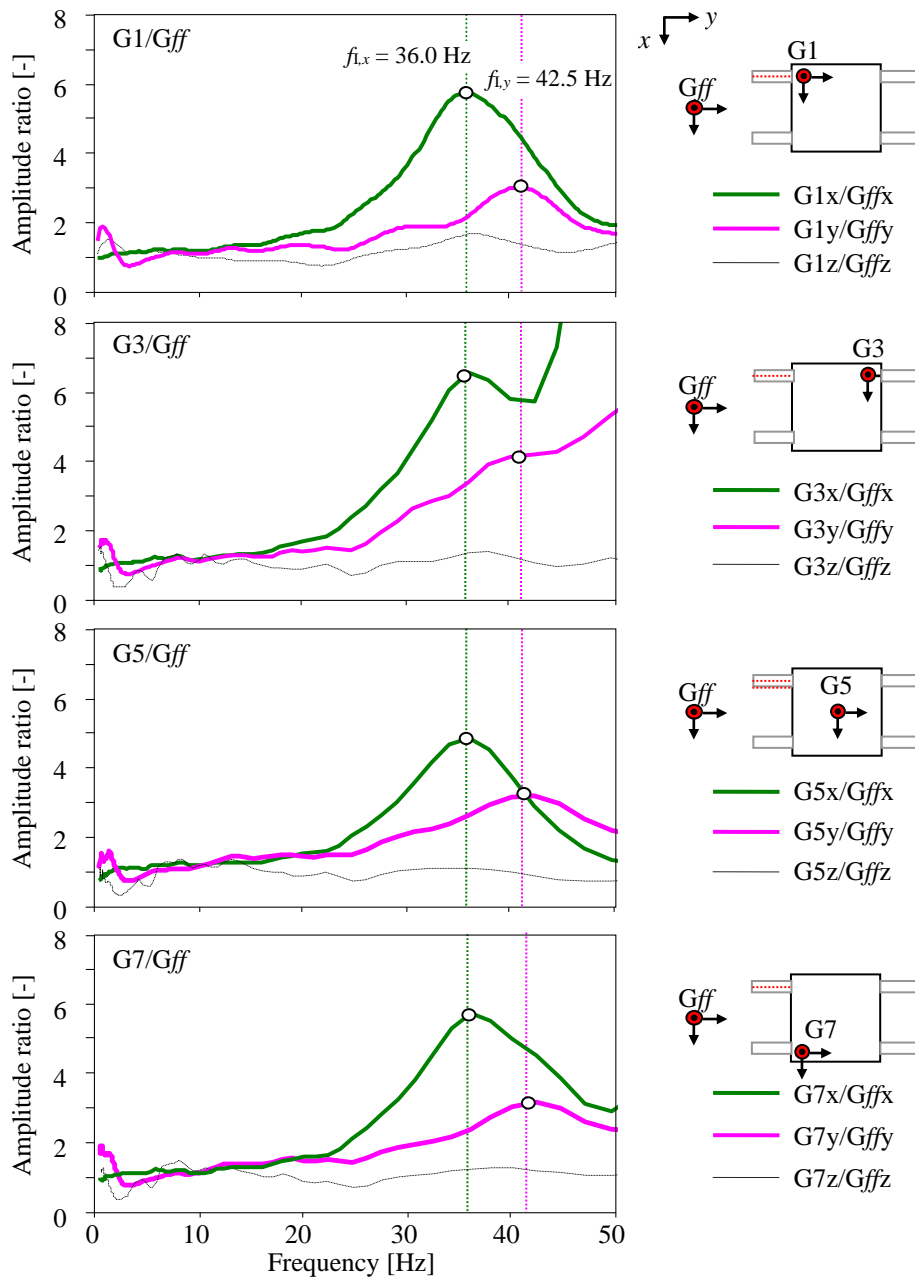


Figure 8. Results of AV tests.

The FV test can be carried out in two different ways, stepped-sine test and sine sweep test. In the stepped-sine testing (used in this work) the command signal supplied to the exciter is a discrete sinusoid with a fixed amplitude and frequency. In order to encompass a frequency range of interest, the command signal frequency is stepped from one discrete value to another in such a way as to provide the necessary density of points for the frequency response plot. For

this technique, it is necessary to ensure that steady state conditions have been attained at each step before the measurements are made.

The vibrator used for FV tests is an electro-mechanical generator of vibrations (vibrodyne), rigidly connected to the structure and able to provide sinusoidal and uniaxial forces (Figure 9a). The acquiring instrumentation, shown in Figure 9b, includes seven accelerometers positioned on the micropile cap and two accelerometers located on the ground surface near the cap ( $g$ ), in addition to the permanent SGs applied on the shaft of one of the inclined micropiles constituting the foundation.

The vibrodyne is characterized by 2 counter-rotating mechanical shafts on which two identical wedge-shaped masses (a mobile mass and a fixed one) are mounted with a certain eccentricity. The mutual angular position of these two masses ( $\alpha$ ) can be regulated when the machine is off. The functioning principle is that the eccentric mass, rotating around an axis with a constant angular velocity  $2\pi f$ , generates a centrifugal sinusoidal force; the amplitude is a parabolic function of the frequency expressed by:

$$|F| = K(\alpha) f^2 \quad (1)$$

where  $K(\alpha)$  is the utilization constant of the machine (hereinafter referred to as  $K$ ) that depends on the masses, their eccentricity from the rotation axis, and the phase angle ( $\alpha$ ) between them.

For the present application, the vibrodyne has a maximum weight of 3.5 kN, the maximum force that can be supplied is 20 kN, while the maximum frequency that can be reached is 50 Hz. Several configurations are considered, by varying the direction of vibration ( $x$  and  $y$  in the global reference system) and the value of  $K$  of the machine (0.9 N/Hz<sup>2</sup>, 4.2 N/Hz<sup>2</sup>, 8.3 N/Hz<sup>2</sup>, 23.4 N/Hz<sup>2</sup>). The set of configurations summarized in Table 3 are carried out: tests indicated with letter b are those that were repeated to check if results were stable. The chronological order of the performed tests is also reported to facilitate the interpretation of results.

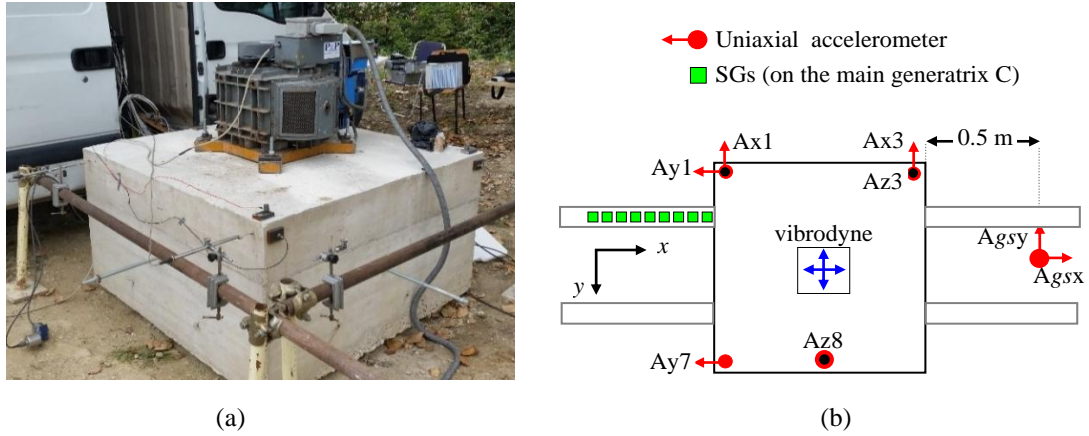


Figure 9. FV tests: (a) vibrodyne positioned on the cap; (b) layout of the acquiring instrumentation.

Table 3. Stepped sine FV tests in chronologic order.

Direction $x$			Direction $y$		
$K$ [N/Hz <sup>2</sup> ]	Test name	Test sequence	$K$ [N/Hz <sup>2</sup> ]	Test name	Test sequence
0.9	FV <sub>x</sub> -0.9a	Ia (day 1)			
0.9	FV <sub>x</sub> -0.9b	Ib (day 1)			
			0.9	FV <sub>y</sub> -0.9a	IIa (day 1)
			4.2	FV <sub>y</sub> -4.2a	IIIa (day 1)
			4.2	FV <sub>y</sub> -4.2b	IIIb (day 1)
4.2	FV <sub>x</sub> -4.2a	IVa (day 2)			
4.2	FV <sub>x</sub> -4.2b	IVb (day 2)			
8.3	FV <sub>x</sub> -8.3a	Va (day 2)			
8.3	FV <sub>x</sub> -8.3b	Vb (day 2)			
23.4	FV <sub>x</sub> -23.4a	VIa (day 2)			
23.4	FV <sub>x</sub> -23.4b	VIb (day 2)			
			8.3	FV <sub>y</sub> -8.3a	VIIa (day 2)
			8.3	FV <sub>y</sub> -8.3b	VIIb (day 2)
			23.4	FV <sub>y</sub> -23.4a	VIIIa (day 2)
			23.4	FV <sub>y</sub> -23.4b	VIIIb (day 2)

As for the acquiring instrumentation, the horizontal accelerations at the ground surface and the vertical accelerations of the cap were acquired by piezoelectric accelerometers ( $A_{gs}$ ) with a

sensitivity of 10 V/g, while horizontal accelerations, which are expected to be higher, are measured through accelerometers having a sensitivity of 100 and 300 mV/g. The external conditioning and amplification of signals acquired by SGs and the vibrodyne was carried out by means of HBM MGC+ signal conditioner. To acquire synchronous signals, the HBM MGC+ conditioner and the accelerometers are finally connected through low-noise coaxial cables to a 24-bit DAQ having an input range of  $\pm 5$  V, connected to laptop with dedicated software.

After each series of tests characterized by the same value of  $K$  along a direction, IL tests along  $x$  and  $y$  axes were carried out on the micropile group to evaluate the “post-shaking” dynamic properties.

Figure 10 shows the results of FV tests in terms of acceleration along the direction of loading  $x$  and  $y$ . Point-by-point FRFs are depicted, relevant to tests performed with increasing values of  $K$ . It is worth noting that resonance frequencies of the first translational modes obtained from the first test (i.e. with  $K = 0.9$ ), producing the lower force on the cap, are lower than those observed by means of IL and AV tests; with respect to the latter, a decrease of about 25% and 15% is observed along  $x$  and  $y$  directions, respectively.

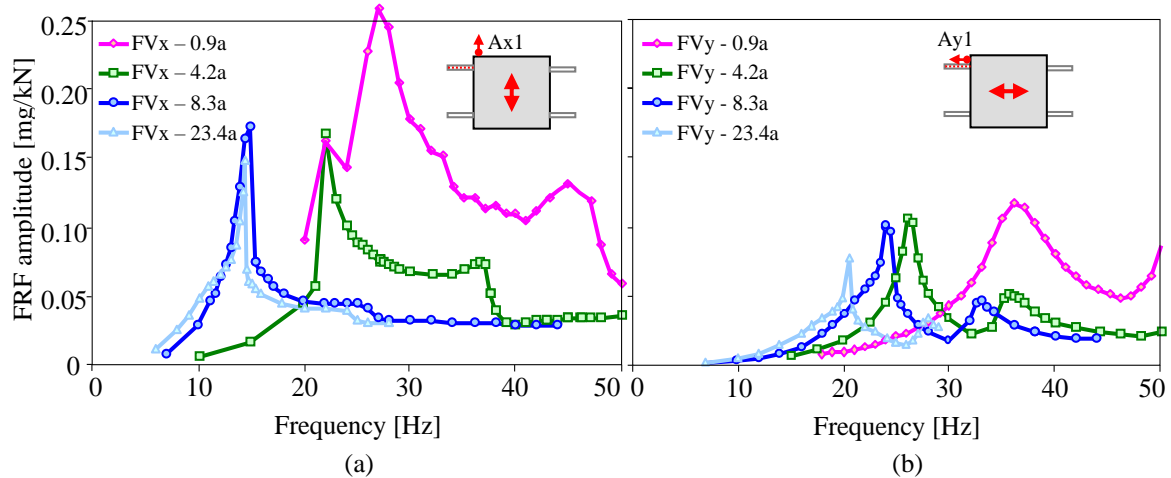


Figure 10. Results of FV tests along (a)  $x$  axis and (b)  $y$  axis for increasing values of  $K$ .

This is due to different reasons including the non-negligible mass of the shaker, which is responsible for a reduction of about 5%, and a first degradation of the system stiffness, consistently with the strain level induced by the FV test, which is higher than that reached during IL and AV tests. In addition, the formation of a superficial “slack” zone of degradation at the soil-micropiles interface due to ambient factors is likely to be occurred. Anyway, consistently with results of previous tests, the fundamental frequency of the first translational mode in  $y$  direction (direction of micropiles inclination) is higher than that relevant to the translational mode in  $x$  direction; at the same time, the first mode in this direction is more damped. By increasing the loading level (i.e. the values of  $K$ ), natural frequencies of the first and second modes (summarized for both directions in Table 4) decrease.

Table 4 Fundamental frequencies from FV tests (tests a).

Configuration	$K = 0.9 \text{ N/Hz}^2$	$K = 4.2 \text{ N/Hz}^2$	$K = 8.3 \text{ N/Hz}^2$	$K = 23.4 \text{ N/Hz}^2$
Direction $x$	27 Hz	22.0 Hz	14.9 Hz	14.4 Hz
Direction $y$	36 Hz	26.6 Hz	24.4 Hz	20.5 Hz

The diminishing of fundamental frequencies can be clearly related to the occurrence of non-linearity in the soil and to the progressive opening of a gap at micropiles-soil interface, that is also responsible for the decrease in the radiation damping. Moreover, with the increasing of  $K$ , FRFs show a peculiar appearance characterized by asymmetrical sharp peaks. In detail, resonance curves of tests FV $_x$ -4.2a, 8.3a and 23.4 a as well as FV $_y$ -8.3a and 23.4 are wide at the base, with a sudden steepening at a certain frequency (related to the development of nonlinear phenomena due to the micropile-soil gap formation and the subsequent reduction of radiation damping), and a vertical collapse once the resonance is reached, which reveals that

the dynamic properties of the system has changed to that of a degraded system characterised by a lower fundamental frequency, as schematized for an ideal problem in Figure 11a.

The peculiar shape of the experimental FRF appears consistent with the theory of the dynamic response of nonideal nonlinear systems subjected to harmonic excitations with increasing frequency (El-Badawy, 2007). From a phenomenological point of view the achievement of the resonance condition (at which the maximum horizontal force is expected) is related to the maximum development of nonlinear phenomena associated to the specific test. Nonlinear degradation phenomena (soil-micropile gap, superficial irregular cracks originating from steel pipes, etc...) concentrate in a radial zone all around micropiles (Figure 11b, c, d).

Finally, it is worth observing that, differently from the  $y$  direction, for which the fundamental frequency of the translational mode always diminishes by increasing the shaking intensity (i.e. the  $K$  values), frequency of the translational mode in the  $x$  direction tends to stabilize at about 14.5 Hz, probably approaching a sort of shakedown condition.

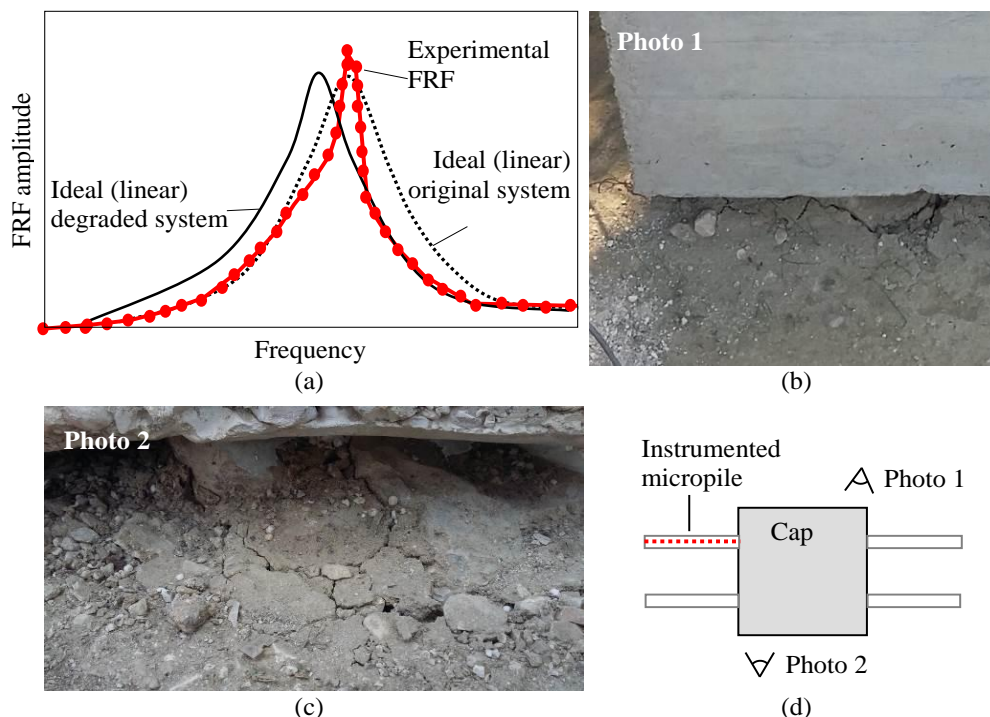


Figure 11. (a) Schematic ideal behaviour vs experimental FRF; (b) and (c) soil cracks around the micropiles observed during FV tests and (d) photos location.

A further interpretation of results is provided in Figure 12 where conditions identified as resonance in Figure 10 are reported in a frequency-force graph, which also includes the tests chronological sequence. Disregarding dynamic amplification effects, this representation allows comparing the maximum exerted levels of force associated to each test. The loading sequence is very important when dealing with non-linear phenomena, because each test influences the result of the subsequent one. First tests were performed by alternating the loading directions ( $x$  and  $y$ ) to investigate the behaviour of the system when excited (although not simultaneously but sequentially) in both directions, like in the seismic case. With the increasing of the force level and the development of strong nonlinear phenomena, the last two tests for each direction were performed sequentially to exclude (at least along the direction of micropiles inclination, which is the one of main interest in this study) any spurious effect induced by the test performed in the orthogonal direction. A clear trend in the Frequency-Force diagram can be identified in the  $y$  direction, while trend relevant to the  $x$  direction is more scattered, presenting a significant change in the resonant frequency without variation of the force intensity between the  $K = 4.2 \text{ N/Hz}^2$  and  $K = 8.3 \text{ N/Hz}^2$  tests. Considering the peculiarity of the chronological order of tests previously addressed, this is due to the degradation induced by the high intensity tests already performed in the orthogonal direction. Moreover, as already observed, the resonant frequency stabilizes around 15-14.5 Hz, probably because the increased force of the last test (VIII) was not able to further damage the soil-micropile interface, subjected to previous significantly high actions in the orthogonal (V and VI) as well as the same (VII) directions.

Figure 13 compares results between two identical tests sequentially performed at low (a) and high (b) intensity force. Results are very similar for FVx-0.9a and b, as expected for a linear system. On the other hand, for what concern FVx-23.4a and b, it can be noted that the achievement of resonance in the second test is substantially different than in the first one, with a characteristics *shark tail* shape for which explanations provided above hold. At low

frequencies (i.e. below the resonance), the resonant curve of the second (b) test (cyan line) is above that of the first (a) one (black line) since it refers to a system degraded by forces reached at the resonant condition in the first test. However, given the high value of the force of the second (b) test, the system is subjected to an additional degradation probably not involving a significant further deepening of the gap (which would be responsible for a sudden steepening of the curve), but producing a reduction of the stiffness and an increase in the material damping of the soil interacting with the micropiles. Accordingly, the resonant frequency slightly decreases and the descending branch of the FRF is translated with respect to that of the first test.

In order to compare the dynamic response of the soil-micropile system in the two principal orthogonal directions, Figure 14 shows results of two subsequent FV tests in the  $x$  and  $y$  directions characterised by a low intensity force ( $K = 0.9 \text{ N/Hz}^2$ ) in terms of point-by-point FRFs of horizontal and vertical accelerations. The tests consequentiality and the low intensity force allow comparing the longitudinal and transverse response at very similar conditions. The roto-translational coupling of the soil-foundation system is clearly evident in the  $x$ - $z$  plane, producing peaks in FRFs of both horizontal and vertical accelerations (Figure 14a).

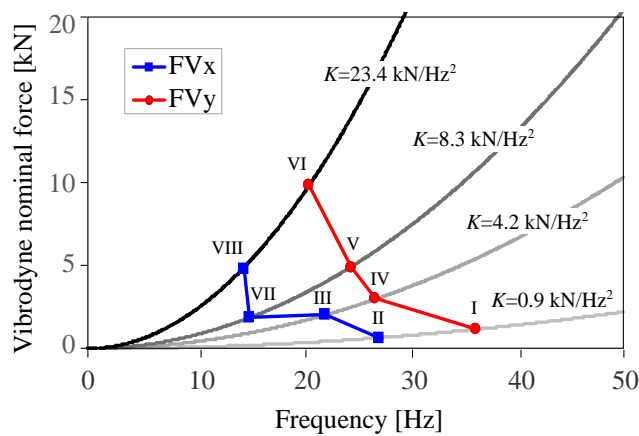


Figure 12. Chronological sequence of FV tests and vibrodyne nominal forces.

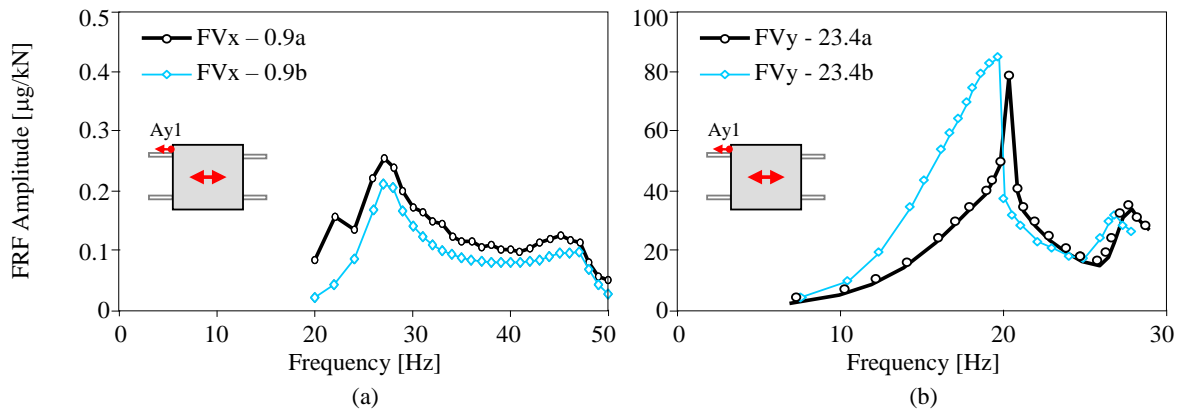


Figure 13. FRFs of two FV tests sequentially performed: (a) low intensity force and (b) high intensity force.

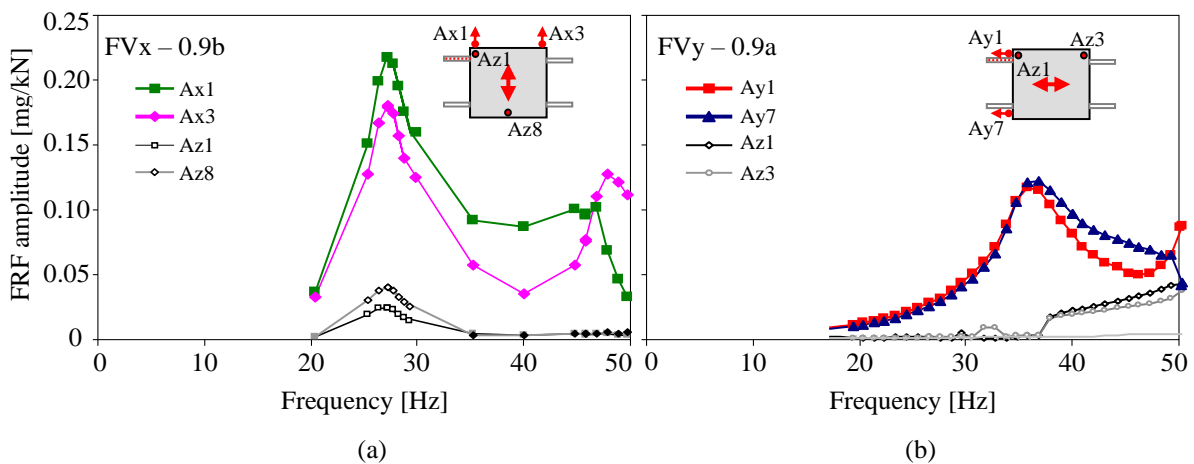


Figure 14. Results of two subsequent FV tests in the x and y directions.

On the contrary, in  $y$ - $z$  plane (where micropiles are inclined) the coupling is not highlighted by a peak in the vertical accelerations, since, as already mentioned in previous sections, the cap rotation is produced by two mutually out-of-phase effects associated to the inertial shear force applied at the top of the cap, and the relevant bending moment (Carbonari et al., 2017). Superposition of the latter effects results in an overall abatement of the FRF peak (Figure 14b). In Figure 15 FRF amplitudes of accelerations acquired on the ground and on the micropile cap along  $x$  and  $y$  axes during FV tests are reported. For the data interpretation, results of AV tests performed in August on the free field (with geophones) are reported in the first row of plots in terms of averaged response spectra, along  $x$  and  $y$  directions. A free-field resonant frequency at about 23 Hz, associated to a superior mode of vibration of the soil deposit, is identified within the range 10 - 50 Hz and denoted in all graphs with a vertical red dashed lined, for each

direction. The subsequent rows of plots contain, for increasing levels of  $K$ , the FRFs of accelerations recorded on the ground and on the cap along the same direction. The black lines on the graphs trace the fundamental frequencies of the excited soil-foundation system for each test.

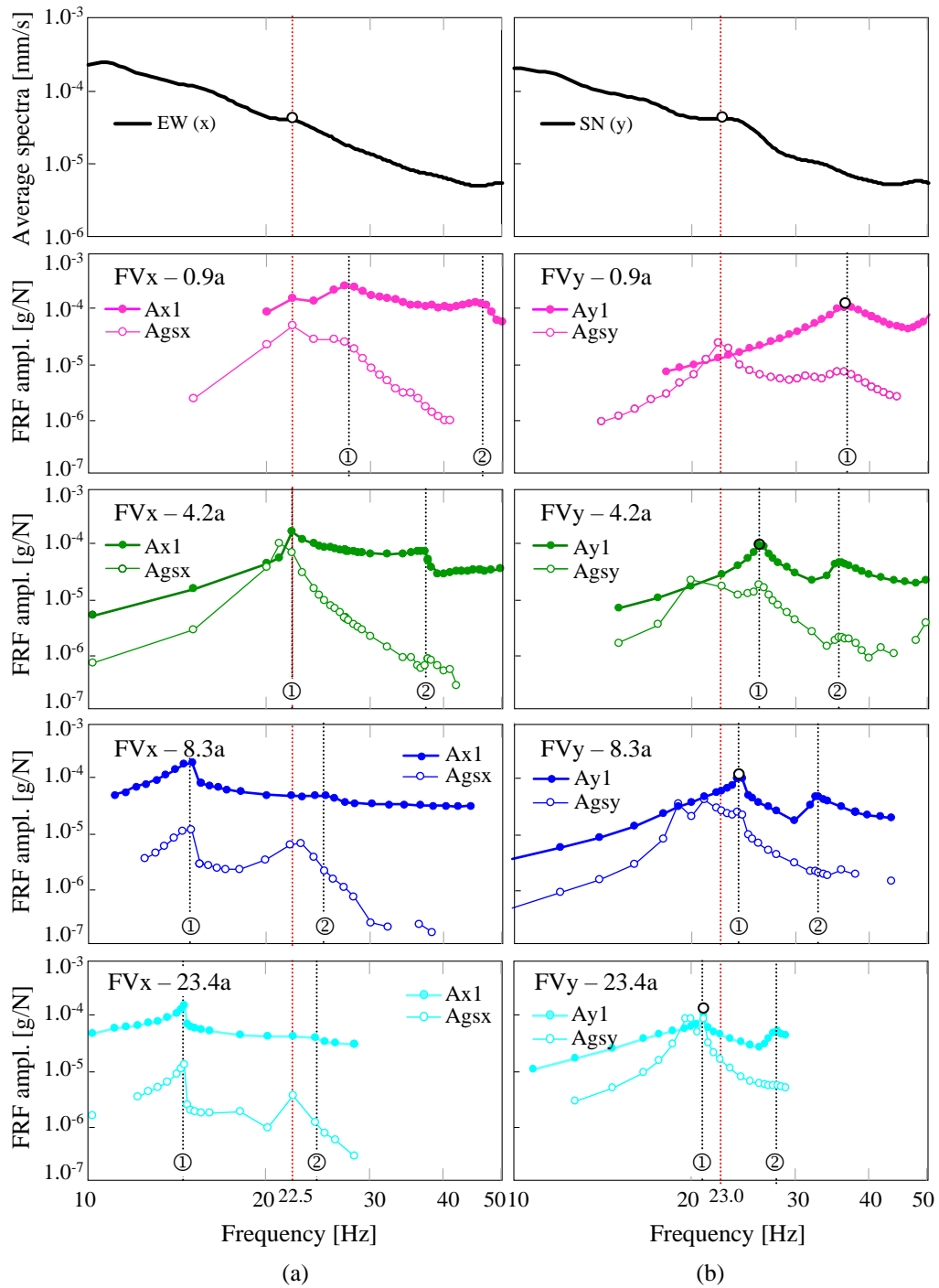


Figure 15. Average spectra of signals by geophones on the free-field (first row) and FRFs of accelerations on the micropile cap and on the ground surface from four FV tests: (a)  $x$  direction and (b)  $y$  direction.

As for the ground response, it is interesting to observe that the FRFs are very often characterized by two or three peaks corresponding to the first and second resonance frequencies of the soil-foundation system (induced by the vibrating system at resonance) and to the deposit resonance frequency (identified at 22.5 Hz and 23 Hz along  $x$  and  $y$  axis, respectively).

This is particularly evident for all the tests in the  $x$  direction, and for the first two levels of dynamic force in the  $y$  direction. For FVy-8.3a and FVy-23.4a, as the fundamental frequency of the soil-foundation system approaches that of the soil deposit, the amplitude of the resonance curve gets comparable to that obtained for the cap (i.e. double resonance condition). This also occurs for test FV $x$ -4.2a.

Moreover, for FVy-8.3a and FVy-23.4a (high force intensity) the shape of the resonance curve for the ground accelerations tends to be more confused and the frequency corresponding to the maximum amplification tends to decrease with respect to that identified by means of AV tests: this can be attributed to the occurrence of nonlinear phenomena developing nearby the measuring point on the ground surface (located 50 cm away from the cap), triggered by the double resonance condition combined with the high level of force intensity.

In Figure 16 FRFs of SG signals recorded on the instrumented micropile during FV tests along  $y$  axis are reported. Figure 16a shows, for a selection of SGs of generatrix C (Figure 3), FRFs at increasing values of  $K$ . By observing FRFs of the same SG for increasing value of  $K$ , the resonance frequency (identified by peaks of FRFs) progressively decreases, consistently with values of Table 4, identified by means of accelerometers on the cap.

SG1, installed near the ground surface, is overall characterized by the highest amplitudes of FRFs with respect to the other ones and, overall, the response of sensors gets less recognizable by increasing the depth. However, SG2 in the last test ( $K = 23.4 \text{ N/Hz}^2$ ) shows a very sharp peak characterized by the most severe value of amplitude.

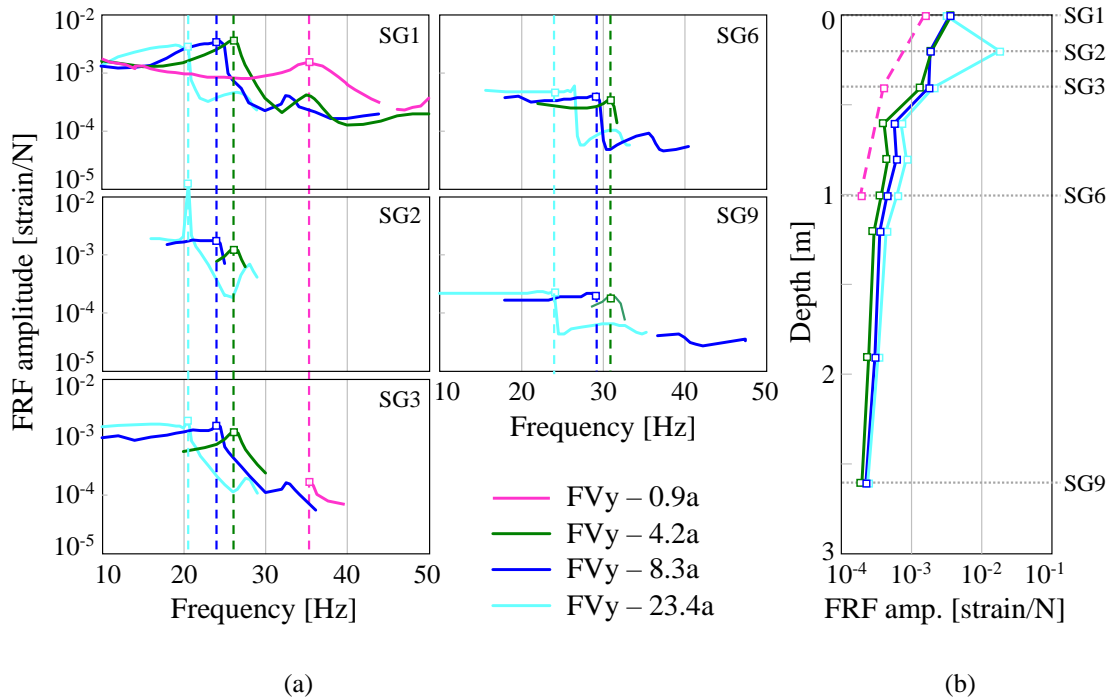


Figure 16. Strains from SGs during FV tests along y direction: (a) FRFs amplitude; (b) maximum strains at resonance along the instrumented micropile.

This peak can be the consequence of the progressive detachment and soil degradation at the interface between the soil and the micropile: by increasing the intensity of the dynamic force, the gap at the soil-micropile interface progressively extends and the depth where a peak in the micropile curvature is expected gets deeper. For low values of  $K$ , that peak, expected to occur between the ground level and 20 cm below, is not observed probably due to the insufficient density of sensors. The peak sharpness, typical of steel members generally characterised by a low damping, is essentially due to the detachment at the interface between the micropile and the soil, and the subsequent reduction of the friction and radiation damping.

Figure 16b shows, for SGs 1 - 9 of generatrix C, the profile of FRF amplitude at resonance for all the level of  $K$ . Overall, the amplitude values tend to increase with the increasing of  $K$ , with exception of the shallower SGs (SG1 and SG2) probably because of the progressive detachment and the superficial degradation of the soil surrounding the micropiles producing a deepening of the cross-section in which maximum strains are achieved.

Finally, Figure 17 shows results of IL tests performed after tests FVy-0.9 (dotted lines) and FVy-23.4b (continuous lines), and after one year the execution of tests (dashed lines). It is worth mentioning that the selected FV tests are those corresponding to the minimum and maximum dynamic force applied to the soil-foundation system and that IL tests are performed after tests b (i.e. after the final test relevant to the specific force intensity). As previously, results are presented in terms of FRFs, namely the ratio between spectra of registered accelerations along  $x$  and  $y$  directions and the input force.

The fundamental frequencies of translational modes of the soil-foundation system, identified through FRFs peaks, and the relevant damping ratios, identified via the half power bandwidth method, are summarized and compared in in Table 5. It is worth mentioning that frequencies obtained from IL tests slightly differ from those directly derived from FV tests reported in Table 4, consistently with the tests procedures from which frequencies are derived (impact intensity is lower than that of FV tests) and with the chronological sequence of tests (data in Table 4 refers to test a). As already observed, a reduction of both the fundamental frequencies and damping ratios is evident for both directions by increasing the intensity of the dynamic loading, due to the development of nonlinear phenomena at the soil-micropile interface (mainly related to the opening of a gap). However, while the frequency reduction is similar in  $x$  and  $y$  directions (about 52-55%), a significant reduction of the damping ratio (about 30%) is only observed in the direction of micropiles inclination (the damping ratio reduction in the direction orthogonal to the micropile inclination is of about 6%). With reference to frequencies evaluated from AV tests, the whole frequency reduction at the end of FV tests is of about 63% and 56% in the  $x$  and  $y$  directions, respectively.

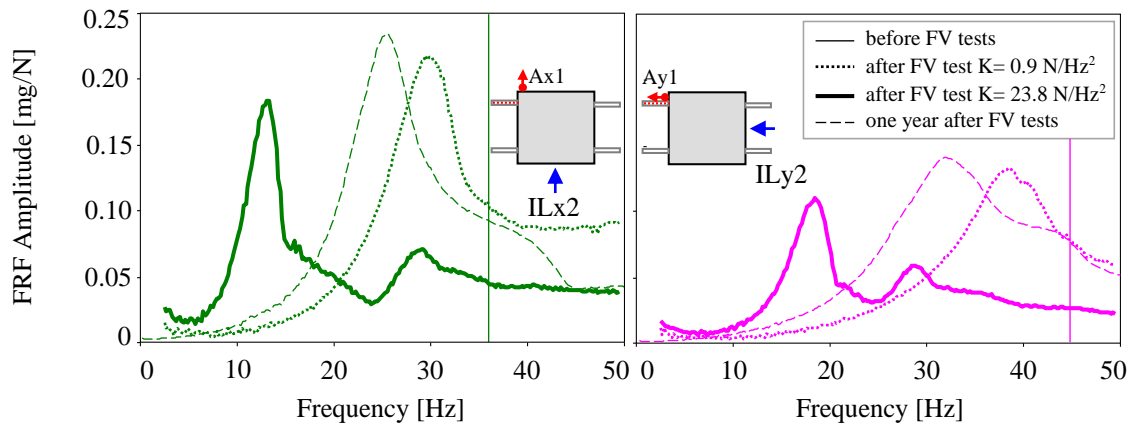


Figure 17. Results of IL tests after FV tests corresponding to the minimum and maximum dynamic forces, and after 1 year from tests: (a)  $x$  direction and (b)  $y$  direction.

Table 5. Degradation and recovery of the soil-foundation system dynamic properties in  $x$  and  $y$  directions

	AV tests before		IL test after FV test		IL test after FV test		IL test 1 year after	
	$x$	$y$	$x$	$y$	$x$	$y$	$x$	$y$
Fundamental frequencies [Hz]	36.0	42.5	29.6	38.6	13.4	18.6	25.6	32.8
Damping ratios [%]	-	-	10.2	10.4	9.6	7.3	11.5	15.1

Accordingly, it can be concluded that the soil-micropile interface degradation, occurring all around micropiles and producing comparable frequency reductions in both directions, compromises largely the dissipation capacity of the soil-foundation system in the direction of micropiles inclination.

Finally, by observing results of IL tests performed one year after the FV tests, a significant increase of both the fundamental frequencies and damping ratios is evident, due to a recovery of the soil-micropile interface probably involving a refilling of the gap. With reference to the system condition before the FV tests, a frequency recovery equals to 71% and 77% of the initial frequencies is observed in the  $x$  and  $y$  directions, respectively.

## 4 Conclusions

An extensive experimental campaign, including ambient vibration, impact load and forced vibration tests carried out on a full-scale group of inclined injected micropiles in transitional silty soils has been presented. Micropiles are inclined in only one direction and tests are performed in both the direction of inclination and the orthogonal one in order to capture effects of the inclination on the system dynamics. Results of tests allow the dynamic characterization of the soil-foundation system in both the small and medium-high strain levels, and permit to observe the evolution of the system behaviour from the linear to the nonlinear field. Both permanent and movable instrumentation, consisting in strain gauges along piles, accelerometers and geophones, is used to measure pile strains as well as the cap and the soil accelerations during the tests. The main features arising from the experimental study are:

- by comparing the behaviour of the soil-foundation system from impact load and ambient vibration tests in the direction of micropile inclination and in the orthogonal one, the contribution of the inclination on the fundamental frequencies of translational modes and the relevant damping ratios can be deduced; in detail, the fundamental frequency in the direction of inclination is about 18% higher than that in the orthogonal direction;
- ambient vibration and impact load tests allow the identification of the complex coupled roto-translational dynamic behaviour of the soil-foundation system. The impact load tests highlighted the peculiar coupled behaviour in the plane containing the inclined micropiles, strongly characterised by the contribution of two out-of-phase effects due to the applied shear force on the cap and the relevant bending moment;

- during forced vibration tests with increasing dynamic forces, several nonlinear phenomena develop at the soil-micropile interface and in the soil surrounding micropiles (e.g. gap opening and slippage at the soil-micropile interface, radial cracks in the soil, materials degradation), producing an overall reduction of the soil-foundation dynamic stiffness; in detail, frequencies of translational modes reduce up to about 60% with respect to values evaluated from ambient vibration tests before the execution of forced vibration tests.
- a reduction of the damping ratios associated to translational modes is observed coherently with the reduction of the system frequencies; this effect, which is more pronounced in the direction of micropile inclination, is reasonably due to the formation of gaps at the soil-micropile interface that determine a reduction of the dissipation capabilities of the system through energy radiation in the soil;
- a significant recovery of the soil-foundation system dynamic properties is observed after one year from tests, probably due to the gap refilling; with reference to frequencies, recovery equals to 77% and 71% of the initial frequencies is observed in the direction of micropile inclination and in the orthogonal one, respectively;
- the nonlinear behaviour observed in the soil-micropile system is coherent with the intermediate nature of the foundation soil, involving both phenomena that are typical for cohesive soils (e.g. gap formation around the micropile shaft) and for granular soils (e.g. the subsequent refilling of the gap with partial recovery of the original dynamic properties).

The experimental campaign included several techniques for the dynamic identification of the investigated soil-foundation systems, commonly not used in practice to test full scale foundations, for which only bearing capacity tests are usually performed. However, dynamic

properties of soil-foundation systems are essential when dealing with soil-structure interaction problems and results of the presented experimental program reveal that ambient vibration tests and impact load tests can provide very stable and reliable information about the fundamental frequency and damping ratios of the system. Forced vibration tests are more complex to be performed but allow investigating the nonlinear behaviour of the piled foundation in the medium-high strain range and can be performed in-situ on pilot foundations for the design optimization. Furthermore, they allow the estimation of the dynamic stiffness of geotechnical systems in the direction of excitation at specific frequency values and force amplitudes.

## **ACKNOWLEDGMENT**

Authors would like to express their deep gratitude to Alseo srl, based in Osimo (AN), for having provided the micropiles and the technical support during all the experimental study, and to PASI srl for having provided some of the instruments; the tireless help of geologists L. Del Maschio and S. Sanchi, are also deeply acknowledged.

## **REFERENCES**

Abd Elaziz AY, El Naggar MH. Group behaviour of hollow-bar micropiles in cohesive soils. *Canadian Geotechnical Journal* 51, 1139–1150 (2014).

AFPS 90. *French association for earthquake engineering*. Recommendations for the redaction of rules relative to the structures and installations built in regions prone to earthquake. Domaine St. Paul – BP.1 – 78470 St Remy les Chevreuses, France (1990).

Bharathi M, Dubey RN, Shukla SK. Experimental investigation of vertical and batter pile groups subjected to dynamic loads. *Soil Dynamics and Earthquake Engineering*, 116, 107-119 (2019).

Bruce DA, DiMillio AF, Juran I. Introduction to micropiles: an international perspective. in Geotechnical Special Publication 1–26 (ASCE, 1995).

Capatti MC, Dezi F, Carbonari S, Gara F. Full scale experimental assessment of the dynamic horizontal behavior of micropiles in alluvial silty soils – *Soil Dynamics and Earthquake Engineering*, 113, 58-74 (2018).

Carbonari S, Morici M, Dezi F, Gara F, Leoni, G. Soil-structure interaction effects in single bridge piers founded on inclined pile groups. *Soil Dynamics and Earthquake Engineering* 92, 52–67 (2017).

Dezi F, Gara F, Roia D. Dynamic response of a near-shore pile to lateral impact load. *Soil Dynamics and Earthquake Engineering* 40, 34–47 (2012).

Dezi F, Gara F, Roia D. Experimental study of near-shore pile-to-pile interaction. *Soil Dynamics and Earthquake Engineering* 48, 282–293 (2013).

Dezi F, Carbonari S, Morici M. A Numerical Model for the Dynamic Analysis of Inclined Pile Groups. *Earthquake Engineering & Structural Dynamics* 45, 45–68 (2016a).

Dezi F, Gara F, Roia D. Linear and Nonlinear Dynamic Response of Piles in Soft Marine Clay. *Journal of Geotechnical and Geoenvironmental Engineering* 04016085 (2016b).

El-Badawy A.A. Behavioral Investigation of a Nonlinear Nonideal Vibrating System. *Journal of Vibration and Control* 13(2): 203– 217 (2007).

El Marsafawi H, Han YC, Novak M. Dynamic Experiments on Two Pile Groups. *Journal of Geotechnical Engineering* 118, 576–592 (1992).

EN1998-5. Eurocode 8: Design of structures for earthquake resistance - Part 5: Foundations, retaining structures, and geotechnical aspects. *Commission of the European Communities, Brussels* (2004).

Escoffier S, Chazelas J-L, Garnier J. Centrifuge modelling of raked piles. *Bulletin of Earthquake Engineering* 6, 689 (2008).

Gerolymos N, Giannakou A, Anastasopoulos I, Gazetas G. Evidence of beneficial role of inclined piles: observations and summary of numerical analyses. *Bulletin of Earthquake Engineering* 6, 705–722 (2008).

Giannakou A, Gerolymos N, Gazetas G, Tazoh T, Anastasopoulos I. Seismic Behavior of Batter Piles: Elastic Response. *Journal of Geotechnical and Geoenvironmental Engineering* 136, 1187–1199 (2010).

González F, Padrón LA, Carbonari S, Morici M, Aznárez JJ, Dezi F, Leoni G. Seismic response of bridge piers on pile groups for different soil damping models and lumped parameter representations of the foundation. *Earthquake Engineering and Structural Dynamics* 48(3): 306-327 (2019a).

González F, Carbonari S, Padrón LA, Morici M, Aznárez JJ, Dezi F, Maeso O, Leoni G. Benefits of inclined pile foundations in earthquake resistant design of bridges. Submitted for review to the journal of *Engineering Structures* (2019b).

Imamura A, Hijikata K, Tomii Y, Nakai S, Hasegawa M. An experimental study on nonlinear pile–soil interaction based on forced vibration tests of a single pile and a pile group. in *Proceedings, 11th World Conference on Earthquake Engineering* (1996).

Juran I, Benslimane A, Hanna S. Engineering analysis of dynamic behavior of micropile systems. *Transportation Research Record* 91–106 (2001).

Kobori T, Miura K, Nakazawa M, Hijikata K, Miyamoto Y. Study on dynamic characteristics of a pile group foundation. (1991).

Novak M, F.Grigg R. Dynamic experiments with small pile foundations. *Canadian Geotechnical Journal* 13, 372–385 (1976).

NTC2018. Aggiornamento delle “Norme tecniche per le costruzioni”. Ministero delle Infrastrutture e dei trasporti. *D.M. 17/01/2018* (2018).

Padrón LA, Aznárez JJ, Maeso O. BEM-FEM coupling model for the dynamic analysis of piles and pile groups, *Engineering Analysis with Boundary Elements* 31(6): 473–484 (2007).

Pender MJ, Hogan LS, Wotherspoon LM. Comparison of Experimental and Computational Snap-Back Responses of Driven Steel Tube Piles in Stiff Clay. 5th Geotechnical Earthquake Engineering and Soil Dynamics Conference: Numerical Modeling and Soil Structure Interaction; Austin; United States; Volume 2018-June, Issue GSP 292, 330-339 (2018).

Priestly N, Singh J, Youd T, Rollins K. *Costa Rica earthquake of April 22, 1991: reconnaissance report*. 7. Earthquake Engineering Research Institute (1991).

Sadek M, Isam S. Three-dimensional finite element analysis of the seismic behavior of inclined micropiles. *Soil Dynamics and Earthquake Engineering* 24, 473–485 (2004).

Sadek M, Shahrour I. Influence of the head and tip connection on the seismic performance of micropiles. *Soil Dynamics and Earthquake Engineering* 26, 461–468 (2006).

SEAOC, Structural Engineers Association Of California. Reflections on the October 17, 1989 Loma Prieta earthquake, Chapter 6 Structural Pounding. *Ad Hoc Earthquake Reconnaissance* (1991).

Sextos A, De Risi R, Pagliaroli A, Foti S, Passeri F, Ausilio E, Cairo R, Capatti MC, Chiabrande F, Chiaradonna A, Dashti S, De Silva F, Dezi F, Durante MG, Giallini S, Lanzo G, Sica S, Simonelli AL, Zimmaro P. Local site effects and incremental damage of buildings

during the 2016 Central Italy earthquake sequence. *Earthquake Spectra* 34(4): 1639-1669. (2018).

Tuzuki M *et al.* Field testing and analysis of dynamic loaded pile group. in *Proc. 10th World Conf. On Earthquake Eng* 3, 1787–1790 (1992).